CRITICAL BEHAVIOR IN $La_{0.7}Sr_{0.3}Mn_{0.98}Cu_{0.02}O_3$ COMPOUND

Le Viet Bau, Trinh Thi Huyen

Received: 20 July 2020/ Accepted: 01 September 2020/ Published: September 2020

Abstract: *The magnetic data of $La_{0.7}Sr_{0.3}Mn_{0.98}Cu_{0.02}O_3$ in the ferro-paramagnetic phase transition region has been analyzed using the Modified Arrott plots (MAP), the Kouvel-Fisher and the scaling hypothesis methods. The obtained data is compared to 4 theoretical models: Mean field, 3D Heisenberg, 3D Ising and Tritical mean field. The results suggest that the magnetic interaction in the sample is corresponding to the 3D Ising model. The n value (which relates to the magnetic order) conducted by law $\Delta S_{max} = a(\mu_0 H)^n$ is 0.641(8). This value is different from 0.556(5) derived from critical exponents of β and γ extracted from fitting values of spontaneous magnetisation and initial susceptibility to Kouvel-Fisher law. A low value of entropy is changed but the relative cooling power is improved.*

Keywords: *Magnetocaloric, critical exponents, manganites, perovskite.*

1. Introduction

The perovskite manganites (La,Sr)MnB'O_3, where B' stands for the transition elements have recently attracted a wide range of research in laboratories because of their potential applications in electric devices that operate based on colossal magnetoresistance effect (CMR) and magnetocaloric effect (MCE) [1-4]. Basically, the magnetic-electronic properties of manganites are explained by the double exchange (DE) interaction. However, it is shown that the ferromagnetic clusters are formed and extracted as decreasing temperature below T_C. This is due to the existence of ferromagnetic clusters above T_C as well as inhomogeneity and phase separation, phase separation phenomenon and lattice distortion effect [5-9]. Those suggest that ferro-magnetic long-range order may be established by percolation of ferromagnetic regions as the temperature is lowered. Such magnetic inhomogeneities in the spin systems may be a result in a reduced local effective topological dimensionality [10], thereby leading to different critical behaviors. The CMR at the paramagnetic-ferromagnetic (PM-FM) transition is explained by the DE interaction [11]. In addition, the low-field-magnetoresistance (LFMR) effect existing in the low temperature region is also promising for application. Hence, the critical properties of the paramagnetic-ferromagnetic (PM-FM) phase transitions in manganites pose an important fundamental problem. On the other hand, the vast variability of competing mechanisms, which may influence the magnetic ordering, may also yield other types of paramagnetic-ferromagnetic transitions for different systems in this class

Le Viet Bau
Chairman of University Council, Hong Duc University
Email: levietbau@hdu.edu.vn (✉)
Trinh Thi Huyen
Inspection Department, Hong Duc University

of materials. Experimental studies [12-14] of the critical behavior of manganites near the PM-FM phase transition by using a variety of techniques have yielded a wide range of values for the critical exponent of β. The values range from about 0.3 - 0.5, which embrace mean-field (β=0.5), three-dimensional (3D) isotropic nearest-neighbor Heisenberg (β=0.365) and 3D Ising (β=0.325) estimates. Static dc-magnetization measurements [12-15], in addition to β, also yield the critical parameters γ and δ for initial susceptibility χ(T) and critical isotherm M(T,H), respectively. However, they may fail to determine a unique universality class for the phase transition of these manganites. The very low values of β=0.095 for $LaMnO_3$ [13] and 0.147 for $La_{0.7}Ca_{0.3}MnO_3$ [14] obtained from static magnetization measurements suggest that the PM-FM transition in these compounds is first-order transition. Further, a first-order PM-FM phase transition has been reported [25] for $La_{0.7}Ca_{0.3}MnO_3$ based on the sign of the slope of the isotherm plots, $(H/M)^{1/\gamma}$ vs. $M^{1/\beta}$ (γ = 1 and β = 0.5 or γ = 1.336 and β = 0.365).

Besides, one of the most important effects is magnetocaloric effect (MCE). Similar to the CMR, MCE occurs with the highest value at ferro-parramagnetic phase transition temperature T_C. Thus it could be related to critical parameters.

In this study, the critical parameters and magnetocaloric of the compound of $La_{0.7}Sr_{0.3}Mn_{0.98}Cu_{0.02}O_3$ were studied. The results are compared with theoretical models to find out intrinsic magnetic interaction in the sample.

2. Experiment

The samples of $La_{0.7}Sr_{0.3}Mn_{0.98}Cu_{0.02}O_3$ were prepared by standard solid state reaction method. The crystal structure, chemical composition of the samples were proved by powder X-ray diffraction (XRD) with D2 Phaser instrument. The X-ray data confirmed that the samples are a single-phase rhombohedral structure with space group R-3c. Magnetic data were collected using a superconducting quantum interference device magnetometer Quantum Design Magnetic Property Measurement System (MPMS).

3. Results and discussions

In order to define the critical parameters from magnetic measurements, M(H), the ferro-parrmagnetic phase transition temperature should be explored.

Figure 1(a) shows the temperature dependence of magnetisation of the sample measured in the applied field of 20 Oe using zero field cooled and field cooled mode. It is shown that in the low temperature, the sample expresses ferromagnetic phase. Parramagnetic phase is formed in the high temperatures. Phase transition behaves a large of the range of temperature. This is a typical behavior of perovskite fabricated by solid state reaction method. The wide of phase transition as well the difference between the zero-field cooled and filed cooled in the range of low temperature does not seem to reflect the chemical disorder but seems due to the disorder in magnetism. It may be in the result of phase separation phenomenon [8].

In order to determine the T_C, the curves of dM/dT vs T has been constructed and shown in Figure 1(b). This figure explores that the T_C is approximately 355 K.

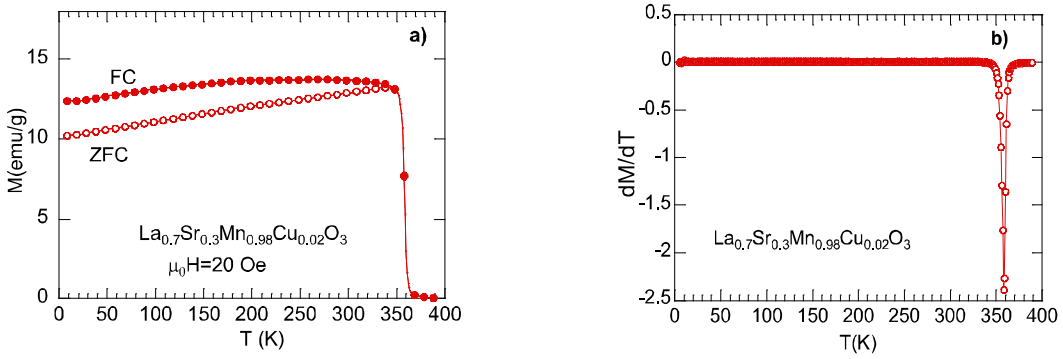

Fig.1. *The magnetization vs temperature in zero-field cooling (empty symbol) and field cooling modes (filled symbol) (a) and the dM_{FC}/dT vs T curve of the sample (b)*

In order to analyze the nature of magnetic interaction near the phase transition, the critical exponents should be explored. The applied field dependence of magnetizations of the samples was measured at several temperatures in the phase transition region. The theorical models are then applied to analyze the experimental data deducted from magnetic measurements.

Figure 2 (a)-(d) display the magnetic data of the samples applied by mean-field (a), 3D-Heisenberg (b), 3D Ising (c) and tricritical mean-field (d) models.

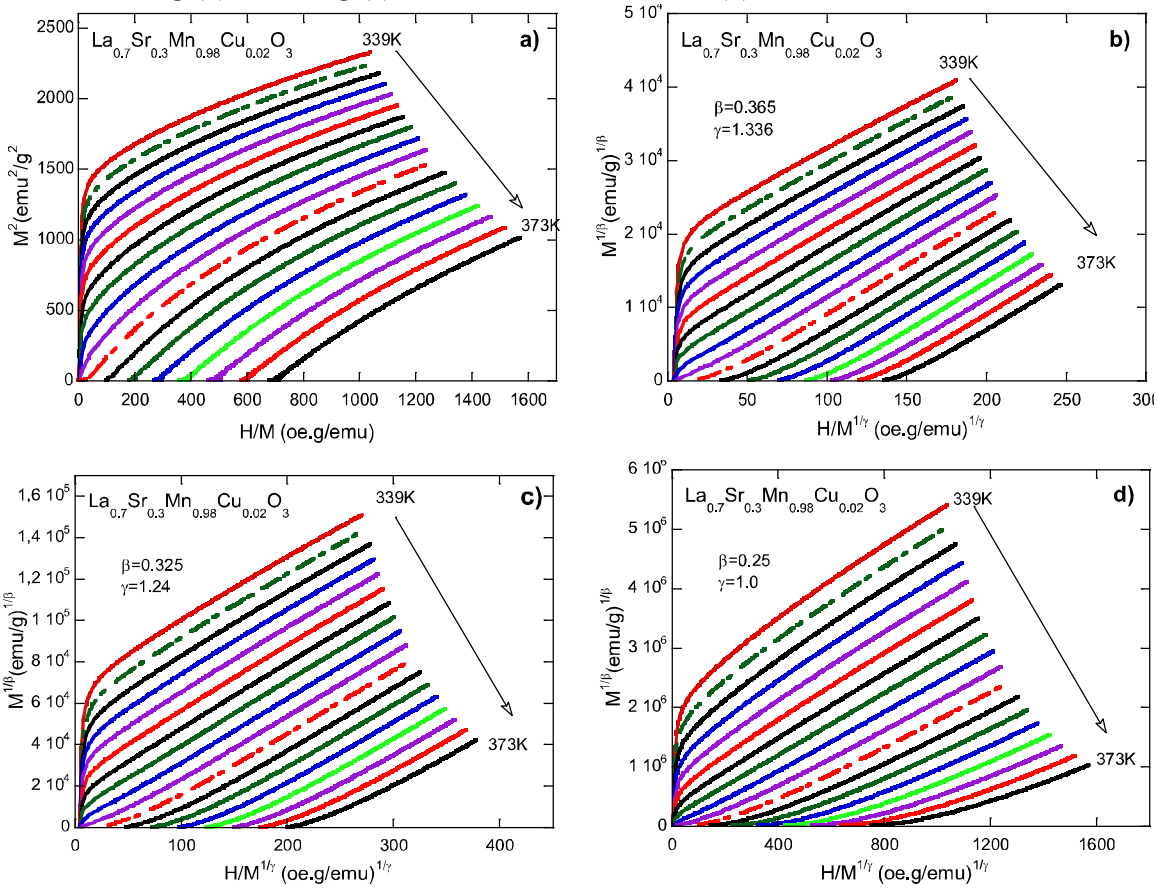

Fig.2. *The isotherm magnetic data of the x=0 sample drew by mean-filed (a); 3D Heisenberg (b); 3D Ising (c); and tricritical mean-field (d) models*

The best model is collected if the curves in the figure are series of straight lines and the line corresponding T_C should pass through the 0. It can be seen from Figure 2, the panel a and d are not collected. The models of 3D Ising (panel b) could be better than the panel c. This could be confirmed using the values of RS defined by RS(T) = $S(T)/S(T_C)$. If the model is suitable, the RS(T) should be 1 [17]. Figure 3 shows the values of RS vs T for the samples.

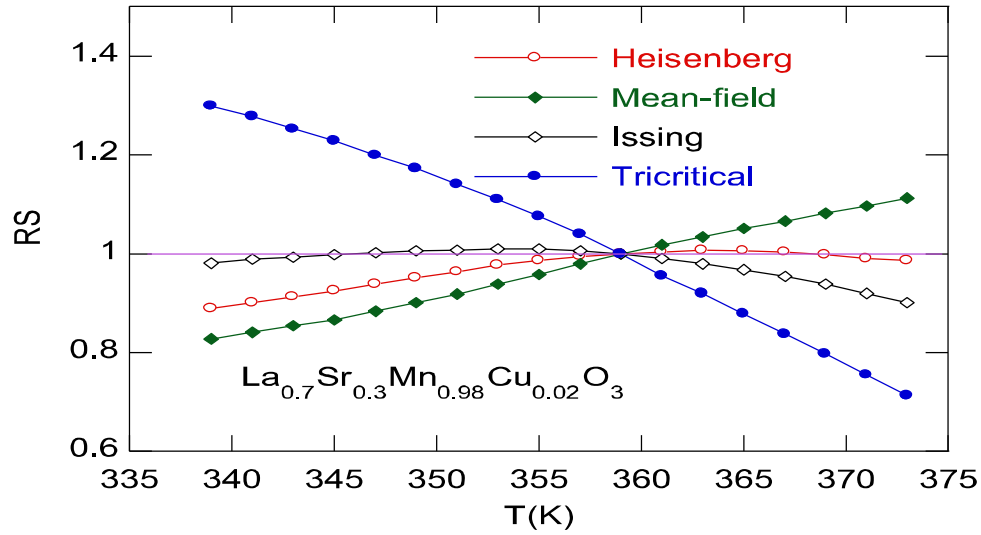

Fig.3. *The values of RS in the 4 models for the x = 0 (a) and x = 0.05 (b) samples*

As can be seen in Figure 3, the RS values diverse from 1 at temperatures far from T_C in all models. However, the best one is 3D Ising model for x = 0 and mean-field model for x = 0.05. Therefore, these models will be applied to analyze the corresponding samples.

In Figure 2, the $(H/M)^{1/\gamma}$ vs $M^{1/\beta}$ curves exhibit a positive slope. According to Banerjee [18], the sample behaves second order magnetic transition (SOMT). For a SOMT, in the range of the ferro-paramagnetic transition temperature, the scaling law was used for the spontaneous magnetisation and initial susceptibility could be described by [19-22]:

$$M_S(T) = M_0 |\varepsilon|^{\beta}, \quad \varepsilon < 0, \quad T < T_C \tag{1}$$

$$\chi^{-1}(T) = (h_0 / M_0)\varepsilon^{\gamma}, \quad \varepsilon > 0, \quad T > T_C \tag{2}$$

$$M = DH^{1/\delta}, \quad \varepsilon = 0, \quad T = T_C \tag{3}$$

With ε is the reduced temperature $(T-T_C)/T_C$. M_0, h_0, and D are the critical amplitudes. The critical parameters β, γ, and δ are critical parameters associated with the spontaneous magnetization $M_S(T,0)$, the initial magnetic susceptibility $\chi(T)$ and critical magnetization isotherm $M(T_C, H)$, respectively. The value of M_S(T) and χ^{-1}(T) deduced from the magnetic data using the 3D Ising model is displayed in Figure 4.

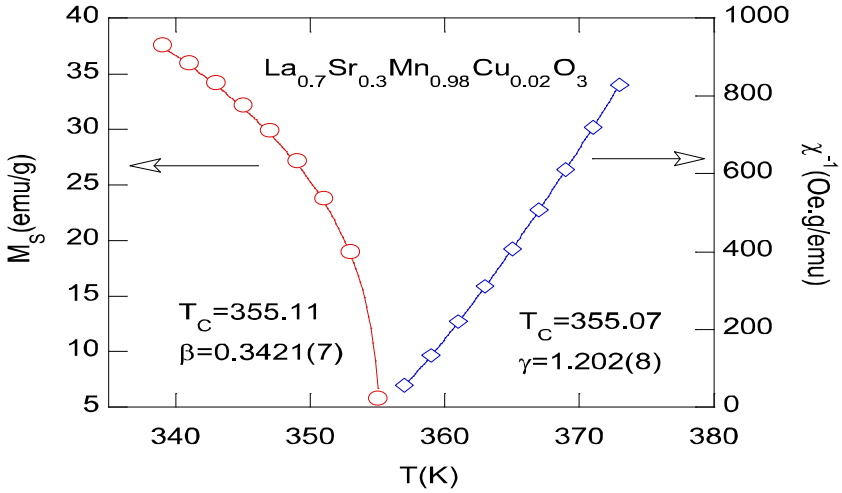

Fig.4. *Temperature dependence of $M_S(T,0)$ and $\chi_0^{-1}(T)$. The lines display the fitting the sample using the power laws*

Figures 4 describes the temperature dependence of $M_S(T)$ and $\chi^{-1}(T)$ of the sample. The curves display the fitting $M_S(T)$ and $\chi^{-1}(T)$ curves to the modified Arrot plots (MAP) to find out the critical exponents. The critical parameters of the sample are defined of β=0.342(1), γ=1.202(8). These values of β and γ are close to those of the 3D-Ising model ($\beta = 0.325$, $\gamma = 1.24$).

Alternately, the critical parameters β, γ and T_C can be determined more accurately by the Kouvel-Fisher (KF) method [18]:

$$\frac{M_S}{\frac{dM_S}{dT}} = \frac{T - T_C}{\beta} \quad , T < T_C \tag{4}$$

$$\frac{\chi - 1}{\frac{d\chi^{-1}}{dT}} = \frac{T - T_C}{T_C} \quad , T > T_C \tag{5}$$

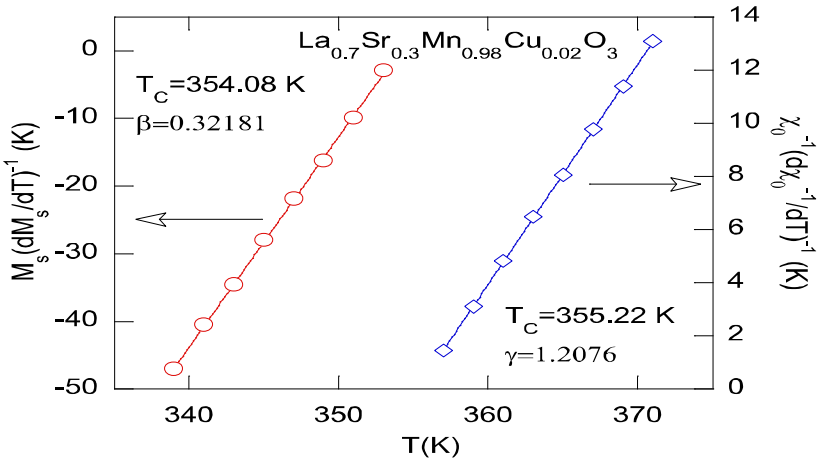

Fig.5. *The temperature dependence of M_S and χ_0^{-1}. The straight lines are fitted to Kouvel-Fisher*

The fitting values of the critical parameters and Curie temperature (T_C) of the samples are also displayed in the same figures. It can be seen that these values are similar to that deducted by fitting experimental data to MAP method.

The value of δ can be deduced using equation (3). The value of T_C is assumed to be mean value of those deduced by equation (2) and (3) as in Figure 5. Thus T_C = 354.65. The M(H) curves at T = 355 K is chosen and displayed in the Figures 6. In the insert panel, the ln(M) vs ln(H) is displayed to find out the value of δ by linear. It can be seen from the insert panel, the data fitting can be seen in Figure 6, when plotted in Ln-Ln scale (the insert figure), the M(H) curves for both samples are straight lines. This could prove that 354K is close to the actual ferro-paramagnetic transition temperatures. It can be seen from the insert of Figure 6, using the formula (3), the LnM - LnH data at $T \approx T_C$ are fitted to determine values of δ. The results show δ = 4.928.

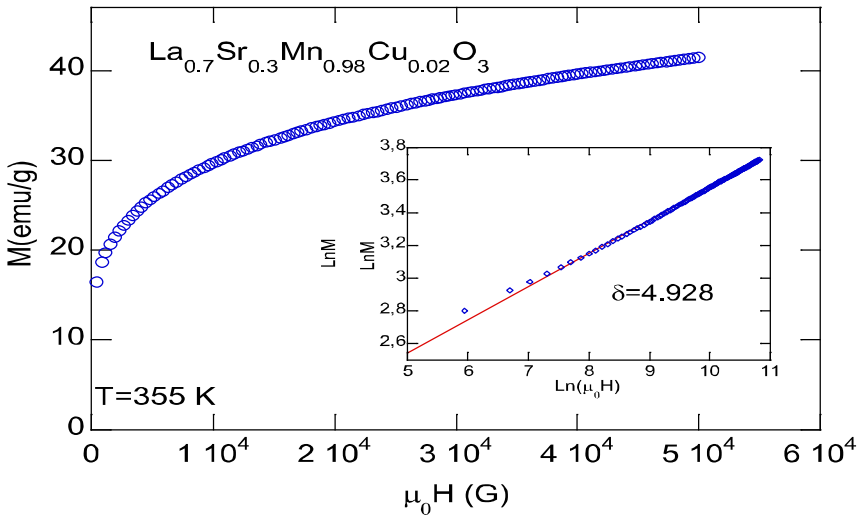

Fig.6. *The applied field dependence of isothermal magnetization measured at T =355 K. The insets display the best fit following Eq. 3*

Moreover, the value of δ can be deducted by Widom scaling relation [24]:

$$\delta = 1 + \gamma / \beta \tag{6}$$

Using values of γ and β obtained by the Kouvel-Fisher method, the value of δ is found to be 4.752(6). The value of δ is slightly different from δ noted in the inserts of Figure 6. Such difference was also observed in several previous studies [25,26] and could due to several reasons such as Jahn-Teller, disorder effects, phase separation phenonmenon, etc., In order to verify the reliability of the exponents and T_C, the scaling hypothesis is contructed. The relation between magnetic isotherms and applied field is described by equation [27]:

$$M(\mu_0 H, \varepsilon) = \varepsilon^{\beta} f_{\pm}(H / \alpha^{\beta+\gamma}) \tag{7}$$

where f_+ and f_- stand for regular functions above and below T_C, respectively.

Eq. (7) suggests that for true β, γ, and δ values, the curves of $M|\varepsilon|^{\beta}$ vs $\mu_0 H/|\varepsilon|^{\beta+\gamma}$ will fall into two identified universal curves above and below T_C. Figure 7 displays the curves of $M|\varepsilon|^{\beta}$ vs $\mu_0 H/|\varepsilon|^{\beta+\gamma}$ with β and γ derived from the Kouvel-Fisher method. The inserts in these figures represent the same plots in the Ln-Ln scale.

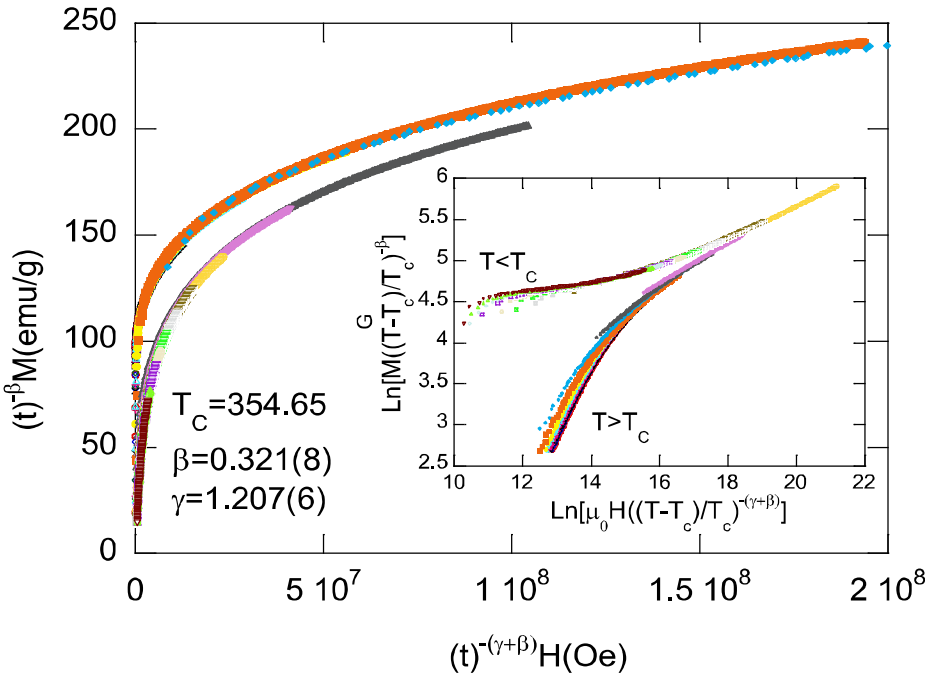

Fig. 7. *Scaling plots* $M|\varepsilon|^{\beta}$ *vs* $\mu_0 H/|\varepsilon|^{\beta+\gamma}$ *of the sample. The plots in log - log scale are represented in the inset*

As can be seen in Figure 7, the M(H, T) in the vicinity of T_C fall into two branches above and below T_C, confirming the reliability of the obtained critical exponents.

The magnetocaloric phenomena was investigated using the applied field dependence of the magnerisation, M(H), at different temperatures. The entropy change at finite temperature is defined by [28, 29].

$$-\Delta S_M\left(\frac{T_1+T_2}{2}\right)=\frac{1}{T_2-T_1}\left[\int_0^H M(T_2,H)dH-\int_0^H M(T_1,H)dH\right] \quad (8)$$

In the case of approximate calculation, it can be calculated by

$$-\Delta S_M\left(\frac{T_1+T_2}{2}\right)=\sum_0^H \frac{\left(\frac{M(T_2,\mathrm{H})-\mathrm{M}(\mathrm{T}_1,\mathrm{H})}{\Delta H}\right)}{T_2-T_1} \quad (9)$$

The result is displayed in Figure 8.

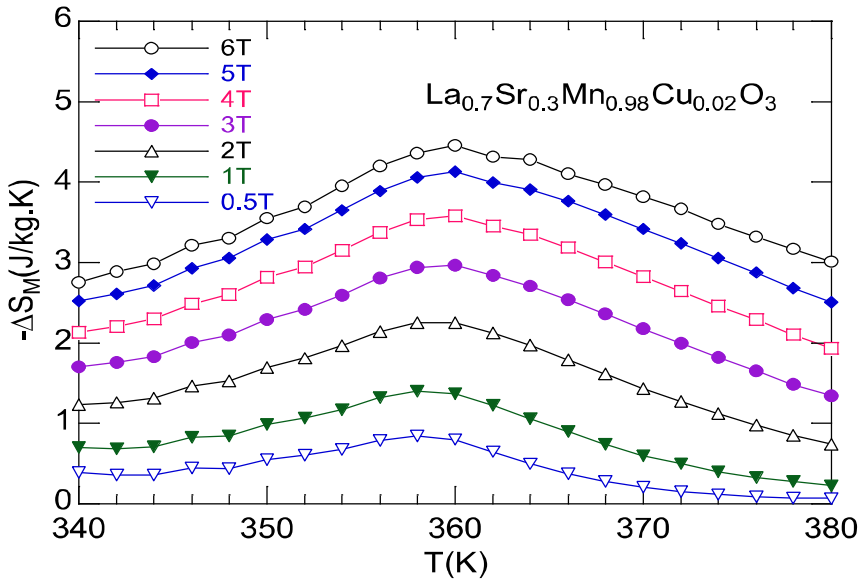

Fig.8. *The MCE of the sample in the difference applied fields*

The magnetocaloric curves are calculated for the applied fields of 0.5T up to 0.7 kg/K. As can be seen from Figure 8, the peaks of those curves shift to the higher temperature in higher applied field. In the low field, magnetocaloric shift to the ferro-paramagnetic transition temperature, T_C=354.65K. This can be understood that the magnetocaloric phenomenon is strongest at the phase transition temperature related to the applied field for the thermo-magnetisation measurements. The shifting of the peaks due to the transition phase temperature is shifted to higher in high applied field. Approximate of 4.5J/Kg.K is the maximum value of magnetocaloric gained in the applied field of 6T. Despite of the small value but it is close to room temperature. It reduces sharply as increasing temperature higher T_C whereas it reduces more slowly in the temperature lowers T_C. This can be explained that in the temperature higher T_C, the material is paramagnetic and it is ferromagnetic in the lowers T_C. It is interesting that the magnetocaloric phenomenon broad over temperature region. This leads to enhancing the range of temperature existing MCE and improves the efficiency of a magnetic refrigerant material or the relative cooling power (RCP).

As mentioned above, the samples are second-order phase transition materials, then the relation between maximum magnetic entropy change and the applied field can be described by a power law $\Delta S_{max} = a(\mu_0 H)^n$ with n is an parameter related to the magnetic order and a is a constant [30].

Figure 11 displays the curve ΔS_{max} vs. $\mu_0 H$ for the sample. The values of the critical exponent n defined by $\Delta S_{max} = a(\mu_0 H)^n$ is 0.641(8). A relationship between n and critical exponents of β and γ is demonstrated by [31]:

$$n(T_C) = 1 + \left[\frac{\beta - 1}{\beta + \gamma}\right] \quad (10)$$

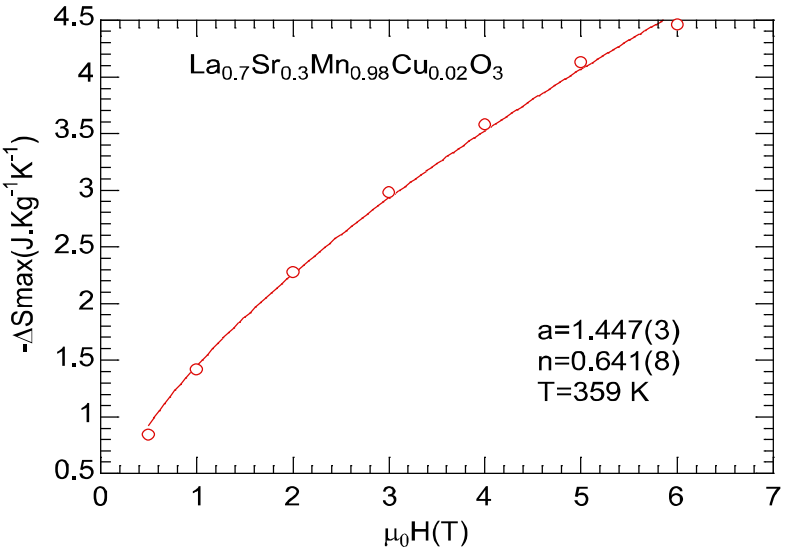

Fig.9. *The maximum of entropy changes vs. the change of the sample. The lines show the best fit to equation* $\Delta S_{max}=a(\mu_0 H)^n$

Using the values of β and γ obtained from the Kouvel-Fisher method and Eq. 13, the values of $n(T_C)$ is found to be = 0.556(5). This value disagrees with the value displayed in Figure 11. This difference was also previously observed in several manganites [25, 32]. The difference between the exponent n deducted from the maximum entropy change and the Kouvel-Fisher method could be caused by the existence of the local inhomogeneities, the superparamagnetic clusters in the vicinity of T_C [23] or the phase separation phenomenon in the samples. In addition, demagnetizing field H_d produced by the material itself could responsible for these differences [33, 34]. Besides, the M(H) curves have been measured in the large range of temperatures and the applied field up to 6T.

4. Conclusion

The critical exponents and magnetocaloric effect of perovskite $La_{0.7}Sr_{0.3}Mn_{0.98}Cu_{0.02}O_3$ has been derived from the isothermal magnetization data. The value of critical parameters β=0.321(8), γ=1.207(6). The value of δ=4.928(1) which is differnent from the value of 4.752(6) reduced from Widom scaling relation. The parameter related to the magnetic order, n, calculated from experimental data and theory is 0.556(5), which is different from 0.641(8) derived from fitting the maximum of entropy change data to $\Delta S_{\max} = a(\mu_0 H)^n$. The differences of the values of δ and n could due to several reasons such as inhomogeneities, Jahn-Teller, or phase separation. The magnetocaloric effect reaches 4.5 Jkg/K in the change of applied field of 6T. The maximum of MCE shifts to the higher temperature in higher applied field change. Although the value of MCE is not high, the relative cooling power is improved.

References

[1] Ramirez (1997), A.P. Colossal magnetoresistance, *J. Phys.: Condens*, *Matter*, 9, 8171.

[2] Phong, P.T.; Bau, L.V.; Hoan, L.C.; Manh, D.H.; Phuc, N.X.; Lee, In-Ja (2015), B-site aluminum doping effect on magnetic, magnetocaloric and electro-transport properties of $La_{0.7}Sr_{0.3}Mn_{1-x}Al_xO_3$, *J. Alloys Compd*, 645, 243.

[3] Dinh Chi Linh, Nguyen Thi Ha, Nguyen Huu Duc, Le Huu Giang Nam, Le Viet Bau, Nguyen Manh An, Seong-Cho Yu, Tran Dang Thanh (2018), Na-doped $La_{0.7}Ca_{0.3}MnO_3$ compounds exhibiting a large magnetocaloric effect near room temperature, *Physica B*, 532, 155.

[4] M'nassri, R.; Chniba-Boudjada , N.; Cheikhrouhou, A. (2015), 3D-Ising ferromagnetic characteristics and magnetocaloric study in $Pr_{0.4}Eu_{0.2}Sr_{0.4}MnO_3$ manganite, *J. Alloys Compd.*, 640, 183.

[5] Teresa J.M. De; Ibarra M.R.; Algarabel P.A.; Ritter, C.; Marquina,C; Blasco, J; Garca, J.; Moral, A. del; Arnold, Z. (1997), Evidence for magnetic polarons in the magnetoresistive perovskites, *Nature* (London), 386, 256.

[6] Uehara, M.; Mori, S.; Chen, C.H.; Cheong, S.-W (1999), Percolative phase separation underlies colossal magnetoresistance in mixed-valent manganites, *Nature* (London), *399*, 560.

[7] Fath, M.; Freisem, S.; Menovsky, A.A.; Tomioka, Y.; Aarts, J.; Mydosh, J.A (1999), Spatially Inhomogeneous Metal-Insulator Transition in Doped Manganites, *Science*, *285,* 1540.

[8] Millis, A.J, Littlewood, P. B. and Shraiman, B. I. (1995), Double Exchange Alone Does Not Explain the Resistivity of $La_{1-x}Sr_xMnO_3$. *Phys. Rev. Lett., 74,* 5144.

[9] Bau, L.V.; Khiem, N.V.;Phuc, N.X.; Hong, L.V.; Nam, D.N.H.; Nordblad, P. (2010), Observation of mixed-phase behavior in the Mn-doped cobaltite $La_{0.7}Sr_{0.3}Co_{1-x}Mn_xO_3$ (x = 0-0.5)*, J. Magn. Magn*. Mater, 322, 753.

[10] Millis, A. J. (1996), Cooperative Jahn-Teller effect and electron-phonon coupling in $La_{1-x}A_xMnO_3$, *Phys. Rev. B*, 53, 8434.

[11] Kaul, S.N (1985), Static critical phenomena in ferromagnets with quenched disorder, *J. Magn. Magn. Mater*, *53*, 5.

[12] Zener, C (1951), Interaction between the d-Shells in the Transition Metals. II. Ferromagnetic Compounds of Manganese with Perovskite Structure, *Phys. Rev*., 82, 403.

[13] Martin, M.C.; Shirane, G.; Endoh, Y.; Hirota, K.; Moritomo, Y.; Tokura, Y. (1996), Magnetism and structural distortion in the $La_{0.7}Sr_{0.3}MnO_3$ metallic ferromagnet, *Phys. Rev. B*, *53*(14), 285.

[14] Freitas, R.S.; Haetinger, C.; Pureur, P.; Alonso, J.A.; Ghivelder, L. (2001), Static critical behavior of the ferromagnetic transition in LaMnO3.14 manganite, *J. Magn. Magn. Mater*, *226-230*, 569.

[15] Shin, H.S.; Lee, J.E.; Nam, Y.S.; Ju, H.L.; Park, C.W. (2001), First-order-like magnetic transition in manganite oxide $La_{0.7}Ca_{0.3}MnO_3$. *Solid State Commun*, *118*, 377.

[16] Hong, C.S.; Kim, W.S.; Hur, N.H. (2001), Transport and magnetic properties in the ferromagnetic regime of $La_{1-x}Ca_xMnO_3$. *Phys. Rev. B*, *63,* 092504.

[17] Mira, J.; Rivas, J.; Rivadulla, F.; Vazquez-Vazquez, C.; Lopez-Quintela,M.A. (1999), Change from first- to second-order magnetic phase transition in $La_{2/3}(Ca,Sr)_{1/3}MnO_3$ perovskites. *Phys. Rev. B*, *60,* 2998.

[18] Belov, K.P. (1965), *Magnetic Transitions*, Boston Technical, Boston.

[19] Banerjee, S. K. (1964), On a generalised approach to first and second order magnetic transitions, *Phys. Lett*, 12, 16.

[20] Kadanoff, L.P.; Gotze, W.; Hamblen, D.; Hecht, R.; Lewis, E.A.S.; Palciauskas, V.V.; Rayl, M.; Swift, J.; Aspnes, D.; Kane, J.(1967), Static Phenomena Near Critical Points: Theory and Experiment, *Rev. Mod. Phys*, 39, 395.

[21] Arrott, A.; Noakes, J.E.(1967), Approximate Equation of State for Nickel Near its Critical Temperature, *Phys. Rev. Lett*, 19, 786.

[22] Fisher, M.E.; Ma, S.-K.; Nickel, B.G.(1972), Critical Exponents for Long-Range Interactions, *Phys. Rev. Lett*, 29, 917.

[23] Arrott, A. (1957), Criterion for Ferromagnetism from Observations of Magnetic Isotherms, *Phys. Rev*, 108, 1394.

[24] Kouvel, J.S.; Fisher, M.E. (1964), Detailed Magnetic Behavior of Nickel Near its Curie Point, *Phys. Rev*, 136, 1626.

[25] Widom, B.(1965), Surface Tension and Molecular Correlations near the Critical Point, *J. Chem. Phys*, 43, 3892.

[26] Le Viet Bau, Nguyen Manh An, Nguyen Le Thi, Le Thi Giang, Tran Dang Thanh, Pham Thanh Phong , Seong-Cho Yu (2019), Critical Exponents and Magnetocaloric Effect in $La_{0.7}Sr_{0.3}Mn_{1-x}$ Ti_xO_3 (x = 0 and 0.05) Compounds, *J. Elec. Materi*, 48, 1446.

[27] Mohamed, Za.; Tka, E.; Dhahri, J.; Hlil, E.K. (2015), Short-range ferromagnetic order in $La_{0.67}Sr_{0.16}Ca_{0.17}MnO_3$ perovskite manganite, *J. Alloys Compd*, 619, 520.

[28] Stanley, H. E.(1971), *Introduction to Phase Transitions and Critical Phenomena*, Oxford University Press, London; pp.1-21.

[29] Földeàki, M.; Chachine, R.; Bose, T.K. (1995), Magnetic measurements: A powerful tool in magnetic refrigerator design, *J. Appl. Phys*, 77(7), 3528.

[30] Amaral, J.S.; Amaral, V.S. (2010), *On estimating the magnetocaloric effect from magnetization measurements*. J.Magn.Magn.Mater, 322, 1552.

[31] Oesterreicher, H. and Parker, F.T. (1984), Magnetic cooling near Curie temperatures above 300 K, *J. Appl. Phys*., 55, 4334.

[32] Franco, V.; Conde, A.; Romero-Enrique, J.M.; and Blazquez, J.S. (2008), A universal curve for the magnetocaloric effect: an analysis based on scaling relations, *J. Phys.: Condens. Matter.*, 20, 28, 5207.

[33] M'nassri, R.; Chniba-Boudjada, N.; Cheikhrouhou, A. (2015), 3D-Ising ferromagnetic characteristics and magnetocaloric study in $Pr_{0.4}Eu_{0.2}Sr_{0.4}MnO_3$ manganite, *J. Alloys Compd*, 640, 183.

[34] Blundell, S. (2014), *Magnetism in condensed matter*, Reprint, Oxford Univ. Press, Oxford.

[35] Hankey, A.; Stanley, H.E. Systematic Application of Generalized Homogeneous Functions to Static Scaling, Dynamic Scaling, and Universality. Phys. Rev. B: Condens. Matter, 6, 3515.